Stokes drift and net transport for two-dimensional wave groups in deep water

T.S. van den Bremer & P.H. Taylor
Department of Engineering Science, University of Oxford
ton.vandenbremer@eng.ox.ac.uk, paul.taylor@eng.ox.ac.uk

Introduction

This paper explores Stokes drift and net subsurface transport by non-linear two-dimensional wave groups with realistic underlying frequency spectra in deep water. It combines analytical expressions from second-order random wave theory with higher order approximate solutions from Creamer et al (1989) to give accurate subsurface kinematics using the H-operator of Bateman, Swan & Taylor (2003). This class of Fourier series based numerical methods is extended by proposing an M-operator, which enables direct evaluation of the net transport underneath a wave group, and a new conformal mapping primer with remarkable properties that removes the persistent problem of high-frequency contamination for such calculations.

Although the literature has examined Stokes drift in regular waves in great detail since its first systematic study by Stokes (1847), the motion of fluid particles transported by a (focussed) wave group has received considerably less attention. Focussed wave groups are relevant, because they can be used to describe the average shape of an extreme wave crest in a random sea (Tromans, Anaturk & Hagemeijer 1991). In practice, the wave field on the open sea often has a group-like structure.

From mass conservation it is clear that Stokes drift by a wave group and Stokes drift by regular waves behave in a fundamentally different way. In fact, the wave-induced Stokes drift and its associated return flow at depth should be locally confined to the wave group and only regular waves (infinite wave trains) can transport mass and momentum indefinitely (McIntyre 1981). Second-order wave theories (e.g. Dalzell 1999) based on the interaction between waves of different frequencies (cf. Longuet-Higgins 1962), predict an irrotational return flow at depth that is equal and opposite to the flow associated with Stokes drift at the surface, as illustrated in figure 1. We show that these results can be extended to higher order by retaining more of the non-linearity of the underlying equations using the results of Creamer et al (1989) with significant additional drift near the focus point.

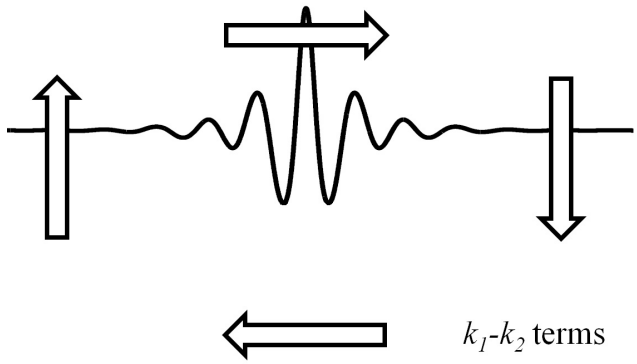

Figure 1: Illustration of the localized irrotational mass circulation moving with the passing wave group. The four fluxes, the Stokes transport in the near surface region and in the direction of wave propagation (left to right); the return flow in the direction opposite to that of wave propagation (right to left); the downflow to the right of the wave group; and the upflow to the left of the wave group, are equal.

Non-linear wave kinematics model

A two-dimensional body of water of infinite depth and indefinite lateral extent is assumed with a coordinate system (x,y), where x denotes the horizontal coordinate and y the vertical coordinate measured from the undisturbed water level upwards. Inviscid, incompressible and irrotational flow is assumed and the usual boundary conditions (kinematic and dynamic at the free surface and a no flow boundary condition at infinite depth) apply. In order to study the drift beneath large waves, we adopt the NewWave wave group of Tromans et al (1991) and set each amplitude term to be proportional to its share in the total discretized wave energy spectrum $S(\omega)$:

$$a_n = a_L \frac{S(\omega_n)}{\sum_{n=1}^{N} S(\omega_n)}, \tag{1}$$

so that the total maximum amplitude is a_L and the shape is that of the auto-correlation function for the sea state. In particular, we consider a (discretized) Jonswap spectrum for fetch-limited seas (Hasselmann, Dunckel

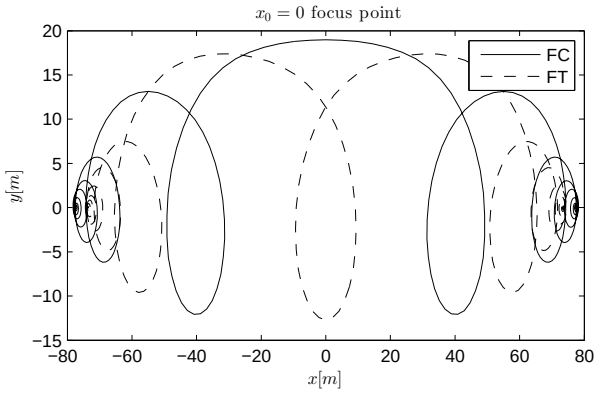

Figure 2: Particles trajectories at the free surface for a focussed wave crest (FC) and a focussed wave trough (FT) with a linear maximum wave amplitude $a_L = 15m$. The particles are at $x_0 = 0$ at the time of focus.

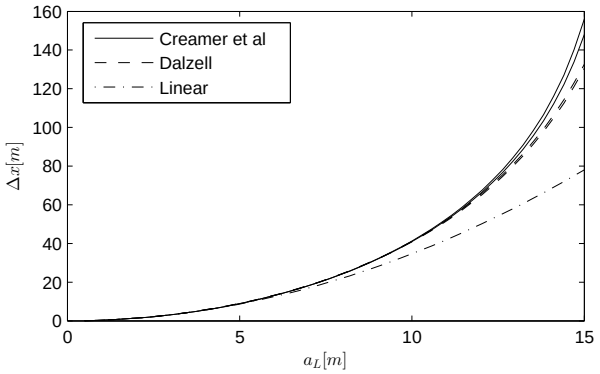

Figure 3: Net horizontal displacement $\Delta x = x(t = -\infty) - x(t = \infty)$ by a wave group travelling past as a function of the maximum linear wave amplitude a_L (i.e. increasing steepness) for focussed crests (top line) and focussed troughs (bottom line).

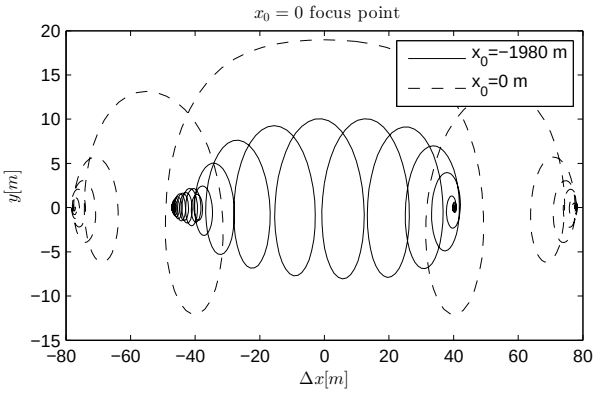

Figure 4: Particles trajectories at the free surface for a focussed wave crest (FC) with a linear wave amplitude $a_L = 15m$ for two different particles located at $x_0 = -1980$ m and $x_0 = 0$ m (focus point) at the time of focus.

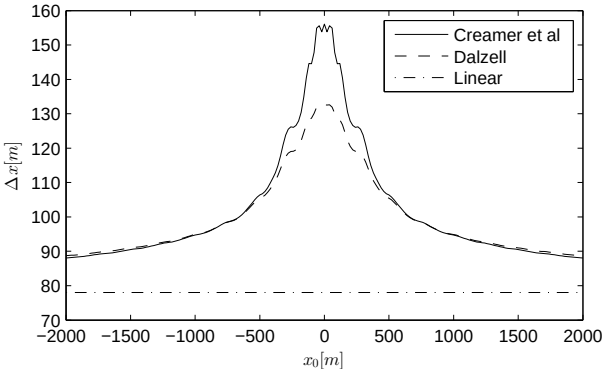

Figure 5: Net horizontal displacement $\Delta x = x(t = -\infty) - x(t = \infty)$ by a wave group with a linear maximum wave amplitude $a_L = 15$ m of particles at the free surface as a function of their location at the time of focus $x_0 = x(t = 0)$.

& Ewing 1980) and we set $T_p = 12.4$ and the peak-enhancement factor $\gamma = 3.3$. A random wave solution to the governing equation and the boundary conditions that is linear in wave steepness ($O(k\eta)$) takes the form:

$$\begin{aligned} \eta_L(x,t) &= \sum_{n=1}^{N} a_n \cos(k_n x - \omega_n t + \mu_n) \\ \phi_L(x,y,t) &= \sum_{n=1}^{N} a_n \omega_n e^{k_n y} \sin(k_n x - \omega_n t + \mu_n), \end{aligned} \tag{2}$$

To include non-linear effects, we rely on the formulation of Creamer et al (1989), who transform the surface elevation η and the surface potential ϕ_s, the two canonical variables that capture the (Hamiltonian) dynamics of the entire problem, into a new set of canonical variables. These new variables exactly reproduce the second-order non-linear behaviour of surface waves and provide a remarkably good approximation to higher-order non-linearity. The nth Fourier component of the transformations of surface elevation η_n and the surface potential $\phi_{s,n}$ on this non-linear free surface are given by (Creamer et al 1989):

$$\begin{aligned} \eta_n &= \frac{1}{|k_n|} \int_{-\infty}^{\infty} \left(e^{ik_n \tilde{\eta}_L(x)} - 1\right) e^{-ik_n x} dx, \\ \phi_n &= \frac{1}{|k_n|} \int_{-\infty}^{\infty} e^{ik_n \tilde{\eta}_L(x)} \tilde{\phi}'_L(x) e^{-ik_n x} dx, \end{aligned} \tag{3}$$

where $\tilde{\eta}_L(x)$ is the Hilbert transform of the linear free surface signal $\eta_L(x)$ and $\tilde{\phi}'_L$ is the Hilbert transform of the spatial gradient of the linear velocity potential.

Conformal mapping

We introduce the following conformal mapping to reduce the steepness of the surface profile to in turn improve the convergence behaviour of the H-operator of Bateman, Swan & Taylor (2003) to calculate subsurface kinematics and eliminate persistent high-frequency contamination

without having to resort to filtering:

$$\xi = z + iA - i\sum_{n=0}^{n=N} a_n e^{-i(k_n z - \omega_n t + \mu_n)}, \qquad (4)$$

where $z = x + iy$ are the complex coordinates in real space and $\xi = \alpha + i\beta$ are the complex coordinates in transformed space. The coefficients a_n and k_n are, respectively, the wave amplitude and the wave number of the first N components of the underlying linear signal. We demonstrate that (4), when applied inversely, for regular waves almost exactly maps a straight line in ξ-space ($\beta = 0$) to the free surface corresponding to a fifth-order Stokes expansion (cf. Fenton 1985) in z-space. For wave groups, the mapping (4) applied inversely maps a straight line into a wavy surface which exactly reproduces the features of a second-order free surface (e.g. Dalzell 1999) excluding the rather small effect of the frequency difference terms.

From the definition of the complex potential $\Psi = \phi + i\psi$, a relationship between the velocities in z and ξ-space can be found:

$$u - iv = \frac{d\Psi}{dz} = \frac{d\Psi}{d\xi}\frac{d\xi}{dz} = \big(u_\alpha - iu_\beta\big)\frac{d\xi}{dz}. \qquad (5)$$

By first mapping to a reduced steepness surface, applying the operators in this space and then mapping back, the persistent problem of high-frequency contamination is effectively eliminated removing the need for inevitably arbitrary numerical filtering.

The M(ass flux)-operator

To directly evaluate the mass flux beneath a given wave profile, we propose a new operator based on the principle of the H-operator of Bateman, Swan & Taylor (2003), which we term the M-operator. The general solution for the velocity potential as a solution to the governing Laplace equation $\nabla^2\phi = 0$ can be given by the sum of N Fourier components (cf. equation 2). From the Cauchy-Riemann equations for an irrotational and incompressible two-dimensional flow field, we have $\partial\phi/\partial x = \partial\psi/\partial y$. The partial derivative of the velocity potential $\partial\phi/\partial x$ can be evaluated from (2) to give a solution for the stream function ψ expressed as an indefinite integral:

$$\psi(x,y,t) = \sum_n^N A_n e^{k_n y}\cos(k_n x - \omega_n t + \mu_n) + f(x,t), \quad (6)$$

where the stream function (6) is now defined up to an arbitrary function of x and t, $f(x,t)$. We can define $\psi_s(x,t) = \psi(x,\eta(x),t) - \psi(x,-\infty,t)$ as the total mass flux (per unit width and with unit density) below the free surface:

$$\psi_s(x,t) = \sum_n^N A_n e^{k_n\eta(x,t)}\cos(k_n x - \omega_n t + \mu_n). \qquad (7)$$

The coefficients A_n and hence the value of the volume flux $\psi_s(x,t)$ can now be obtained from a procedure (the M-operator) similar to the H-operator of Bateman, Swan & Taylor (2003). Making use of the properties of the complex potential across conformally mappable spaces, the M-operator can be applied in ξ-space to avoid high-frequency contamination and ensure convergence.

Result 1: Stokes drift

As the particles undergoes its otherwise circular motion, two factors contribute to Stokes drift at the free surface: deviation from the still water level $z = 0$ and deviation from the initial horizontal position x_0. Using linear kinematics, the net horizontal displacement by a passing wave group $\Delta x = x(t = \infty) - x(-\infty)$ of a particle at the surface can thus be obtained by integrating the horizontal velocity $u(x,\eta(x,t),t)$ with respect to time:

$$\Delta x = \int_{-\infty}^{\infty}\frac{dx}{dt}dt = \sum_{n=1}^{N}\frac{a_n^2\omega_n k_n}{2}T^* + O(\epsilon^3), \qquad (8)$$

where $T^* = 2\pi/\Delta\omega$ is the repeat period of the discretized (with intervals $\Delta\omega$) frequency spectrum [1] and only up to second-order in wave steepness are included.

By numerically solving the two simultaneous differential equations for the position of a particle that is initially at the surface (and thus stays there):

$$\frac{dx}{dt} = u(x,y,t), \quad \frac{dy}{dt} = w(x,y,t), \qquad (9)$$

we also evaluate the Stokes drift in a framework in which kinematics are described by Dalzell's (1999) second-order wave theory and the Creamer transform. Figure 2 traces out the orbital paths that are described by a particle that is located at the focus point at the time of focus $t = 0$ for a focussed crest and a focussed trough based on the non-linear kinematics obtained from the Creamer transform. A large part of the transport is performed by just a few large orbits close to the focus point, where the surface elevation is large and the waves are at their most non-linear.

Figure 3 then compares the net horizontal displacement by a passing wave group Δx of a particle at the surface located at the focus point at the time of focus calculated by three different methods: the analytical expression based on linear wave theory (8) and the numerical solutions based on Dalzell's (1999) second-order random wave theory and the Creamer transform. It is evident from this figure that the horizontal displacement in-

[1] Note that (8) is not a function of the number of components N as N becomes large. To see this, note $a_n \sim N^{-1}$ and $T^* \sim N$ resulting in the individual terms in the sum (8) to behave as N^{-1}. Summing over all the N terms then cancels the dependency on N.

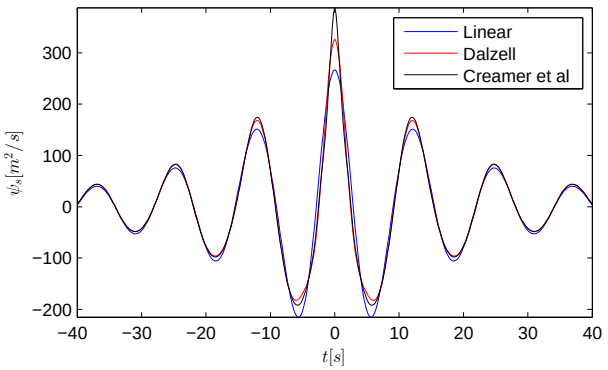

Figure 6: Net depth-integrated mass flux at the focus point as a function of time evaluated from linear theory, using the second-order random wave theory of Dalzell(1999) and the M-operator applied to the more non-linear signal obtained from the Creamer transform ($a_L = 15$ m).

creases with increasing wave amplitude and hence, keeping the other parameters of the spectrum fixed, increasing wave steepness and that non-linear effects are important.

It is evident from (8) that displacement predicted based on linear theory is not a function of the initial position of the particle. Close to the focus point, the net displacement will be produced by a few large orbits, whereas away from the focus point, where the wave group is dispersed, the equivalent net displacement is produced by a large number of small orbits. Comparing, on the other hand, the trajectories of two particles, one located at the focus point at the time of focus and one very far away from it, obtained from the non-linear kinematics and surface elevation through the Creamer transform, figure 4 shows very different behaviour. Clearly, a particle at the focus point at the time of focus is transported further mainly by one or two large orbits corresponding to the highest few peak of the wave group. Figure 5 shows the net displacement Δx as a function of the position of the particle at the time of focus x_0 confirming an additional drift effect for particles within $\sim \pm 2\lambda_p$ of the focus point at the time of focus, where here $\lambda_p \approx 240$ m. For a relatively steep wave considered herein (cf. $k_p a_L \approx 0.39$), the net displacement Δx in this region is approximately two times the net displacement predicted by linear theory.

Result 2: Return flow and net transport

One of the fundamental properties of wave groups is that the surface elevation returns to the still water $\eta(x) \to 0$ as $x \to \pm\infty$. The same applies to the kinematics. In fact, close to focus, non-zero surface elevation and kinematics are confined to $\approx \pm 4\lambda_p$ of the focus point. The transport of fluid in the direction of wave propagation by Stokes drift at and near the surface must therefore be compensated by a return flow at depth in the opposite direction to ensure conservation of mass. Creamer et al (1989), albeit only for a narrow-banded wave group, show that this is indeed the case for the non-linear wave profile obtained using their transform. For second-order random wave theories, the frequency difference terms $(k_1 - k_2)$ of the horizontal velocity are responsible for this return flow. These terms have a repeat period of $(2\pi/\Delta\omega)$, where $\Delta\omega$ is the interval of the discrete frequency spectrum. In the limit $\omega \to 0$, which corresponds to an infinite number of representative Fourier components $N \to \infty$ and the limit in which the wave group is truly localized and not periodic with a very long repeat period, these terms therefore correspond to a net flow, which only decays very slowly with depth (cf. $exp(|k_1 - k_2|y)$).

The M-operator is applied in figure 6 showing the zero-mean depth-integrated mass flux underneath a focussed crest from linear theory, Dalzell (1999) second-order random wave theory and the Creamer transform as a function of time. It is evident from this figure that non-linear effects account for a larger local transport of mass by the largest crest, which is compensated by a greater return flow underneath the troughs. A second feature is that the time integral of the depth-integrated flux for all cases is zero, to within the numerical accuracy of the computations, as would be expected from continuity.

References

Bateman, W.J.D., Swan, C. & Taylor, P.H., 2003. On the calculation of the water particle kinematics arising in a directionally spread wavefield. *J. Comput. Phys.* **186**, 70-92.

Creamer, D.B., Henyey F., Schult, R. & Wright, J., 1989. Improved linear representation of ocean surface waves. *J. Fluid Mech.* **205**, 135-161.

Dalzell, J.R., 1999. A note on finite depth second-order wave-wave interactions. *Appl. Ocean Res.* **21**, 3, 105-111.

Fenton, J.D., 1985. A fifth-order Stokes theory for steady waves. *J. Waterway Port Coastal and Ocean Engineering*, **111**, 216-234.

Hasselmann, D.E., Dunckel, M., Ewing, J.A., 1980. Directional Wave Spectra Observed during JONSWAP 1973. *J. Phys. Oceanogr.*, **10**, 1264-1280.

Longuet-Higgins, M.S., 1962. Resonant interaction between two trains of gravity waves. *J. Fluid Mech.*, **12**, 321-332.

Mcintyre, M.E., 1981. On the 'wave momentum' myth. *J. Fluid Mech.*, **106**, 331-347.

Stokes, G.G., 1847. On the theory of oscillatory waves. *Trans. Camb. Philos. Soc.* **8**, 441-455. Reprinted in: Stokes, G.G. (1880). Mathematical and Physical Papers, Volume I, Cambridge University Press. 197-229.

Taylor, P.H., 1992. On the kinematics of large ocean waves. *Proceedings 6th International Conference of the Behaviour of Offshore Structures (BOSS.)* **1**, 134-145.

Tromans, P.S., Anaturk, A.H.R., Hagemeijer, P.M., 1991. New model for the kinematics of large ocean waves - application as a design wave. *Proceedings of the 1st International Offshore and Polar Engineering Conference*, 64–71.